Electron-phonon scattering in cold-metal contacted two-dimensional semiconductor devices

Rutger Duflou[1,2], Michel Houssa[1,2], and Aryan Afzalian[1]
[1] imec, Kapeldreef 75, 3001 Leuven, Belgium
[2] KU Leuven, Dept. of Physics and Astronomy, Celestijnenlaan 200 D, 3001 Leuven, Belgium
rutger.duflou@imec.be

***Abstract*—Using our DFT+NEGF code, we confirm previous work which shows that cold metal contacted transistors based on 2D materials can achieve subthreshold swings lower than the thermionic limit. This is, however, only true in the ballistic limit and is negated by scattering effects. Additionally, symmetrically connected devices suffer from degraded on-current which increases with increased source-drain bias due to reduced overlap of the energy windows of available states at source and drain.**

***Index Terms*—semiconductor device modelling, cold metals, metal-semiconductor interfaces, NEGF, 2D materials**

I. Introduction

The class of two-dimensional (2D) materials is an interesting candidate for next-generation ultra-scaled devices. Their minimal channel thickness due to their two-dimensional nature results in excellent electrostatic control by the gate which could counter certain short channel effects [1], [2]. Additionally, 2D materials are predicted to be the more resilient against device variation and surface defects and roughness due to their uniform thickness and lack of out-of-plane bonds [3], [4]. However, even if the electrostatic control were perfect, 2D materials are still limited by the thermionic limit of $60\,\mathrm{mV/dec}$ which puts constraints on the operating voltage V_{dd} for fixed I_{ON}/I_{OFF}-ratio [5]. An interesting candidate to circumvent the constraints posed by the thermionic limit, can be found in the class of cold metals [6]. Cold metals have no or limited high-energy states, meaning there is limited injection of carriers at energies high enough to cross the channel barrier in off-state. Previous research [6] has shown, using a combination of density functional theory (DFT) and the non-equilibrium Green's function (NEGF) formalism for transport characteristics, that cold-metal contacted transition-metal chalcogenides (TMDs) can achieve subthreshold swings (S_{th}) much lower than $60\,\mathrm{mV/dec}$. However, this work, and indeed most work based on NEGF, operates in the ballistic limit, where scattering due to electron-phonon interactions is neglected. Our NEGF code, ATOMOS [7], allows us to incorporate the effect of electron-phonon scattering. In Section II, we discuss the modelling choices made within our NEGF framework. In Section III, we look at simulation results of several semiconductor devices with different cold-metal contact configurations.

Funded by the FWO as part of the PhD fellowship 1100321N

978-1-6654-0685-7/21/$31.00 ©2021 IEEE

II. Simulation specifications

DFT is a well-established simulation technique to extract electronic and thermodynamic properties of materials, such as 2D materials. However, as DFT inherently simulates materials in equilibrium, it cannot be used for transport in devices. The NEGF framework [8] allows one to simulate transport in devices and incorporate scattering by electron-phonon interaction. ATOMOS operates in a DFT+NEGF framework, where DFT is used to extract the electronic states present in the material. These states are then converted to orbital-like maximally localized wave functions (MLWFs) using Wannier90 [9]. The Hamiltonian matrix, expressing the interactions between these wave functions, is loaded in ATOMOS. ATOMOS then applies the NEGF formalism using these Hamiltonian matrix elements. The complete procedure is explained in more detail in [10]. In this work, we focus on NbS_2 and WS_2 van der Waals heterojunctions as contacts. Van der Waals heterojunctions are predicted to be resilient to Fermi-level pinning due to the lack of dangling bonds at the interface. P-type WS_2 transistors have been shown to allow excellent ON current [10] and NbS_2 is a cold metal with both a large and small band gap at energies, respectively, higher and lower than the Fermi level, as shown in Fig. 1 (a).

A. DFT+Wannier

The DFT simulations were performed with Quantum Espresso [11] and consisted of a relaxation for NbS_2 and WS_2 with variable cell dimensions, straining both by 2.4% to match the lattice parameters and then a second relaxation of the atomic positions, as described in [12]. The OptB86 functional was used in combination with ultrasoft pseudopotentials and the Grimme DFT-D3 van der Waals correction with a $30\,\text{Å}$ vaccuum between cells. The energy cut-off for the planewave basis was put at 75 Ry and a $8{\times}8{\times}1$ Monkhorst-Pack grid was used, which was found to be sufficient to achieve a relative error on the total energy of less than 10^{-6}. The self-consistency convergence criterion was set to 10^{-6} eV and the atomic force convergence criterion was set to 10^{-3} eV/Å. Finally the Wannier90 package was used to extract the MLWFs and corresponding Hamiltonian elements, starting from 3 p orbitals on S and 5 d orbitals on W and Nb.

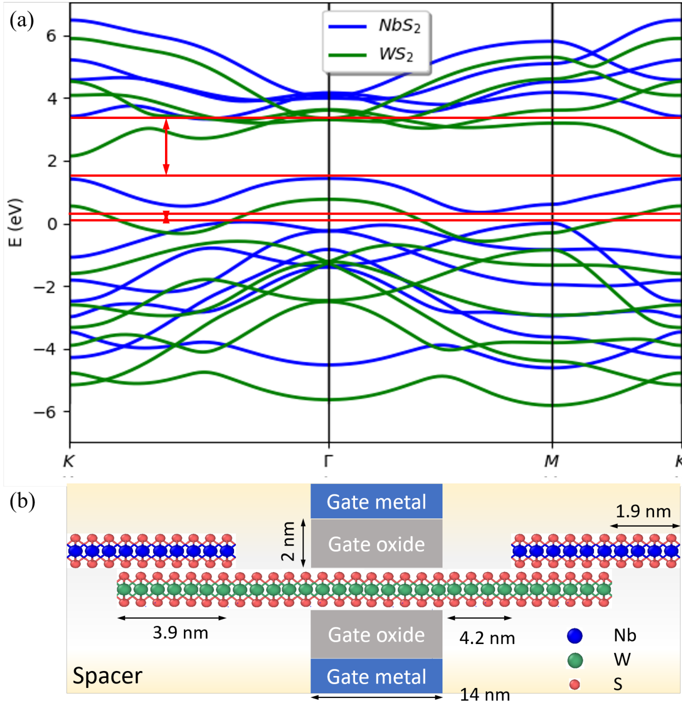

Fig. 1. The material and device parameters. (a) shows the band structures of WS_2 and NbS_2. The red arrows indicate the band gaps of NbS_2. (b) denotes the device dimensions. The left and right part denote respectively the source and drain region. Each comprises of a pure NbS_2 metallic part contacted to the environment through an ohmic contact, an overlap region which forms the metal semiconductor top contact, and a pure WS_2 source-drain extension.

B. ATOMOS

ATOMOS operates by building a full atomistic device with a device Hamiltonian, for which the matrix elements are extracted from the material Hamiltonian. The dimensions of our dual-gated transistor, are denoted in Fig 1 (b). The doping levels in the source and drain extensions are set to $1.9 \cdot 10^{13}$ cm^{-2}, 10 k-points on half the Brillouin zone are used in the periodic direction and the effective oxide thickness is chosen to be $0.5\,\mathrm{nm}$.

III. Results

We simulated the device in Fig. 1 for several source-drain and source-gate bias conditions. For reference, we also simulated the device without explicitly incorporating the metal contacts, i.e., the metal parts where removed and the semiconducting parts were extended to achieve the same device dimensions. The device was then contacted to the environment through ohmic contacts within the semiconducting regions. Finally, we also simulated the device with the metal only explicitly incorporated at the source side and with the drain side metal part replaced by an ohmic contact. The results for $V_{dd} = 0.15\,\mathrm{V}$ are denoted in Fig. 2. From the log scale it is immediately clear that in the ballistic limit, a subthreshold swing much lower than the thermionic limit of $60\,\mathrm{mV/dec}$ is found, namely $\sim 20\,\mathrm{mV/dec}$. When electron-phonon interaction is taken into account, scattering with phonons can grant

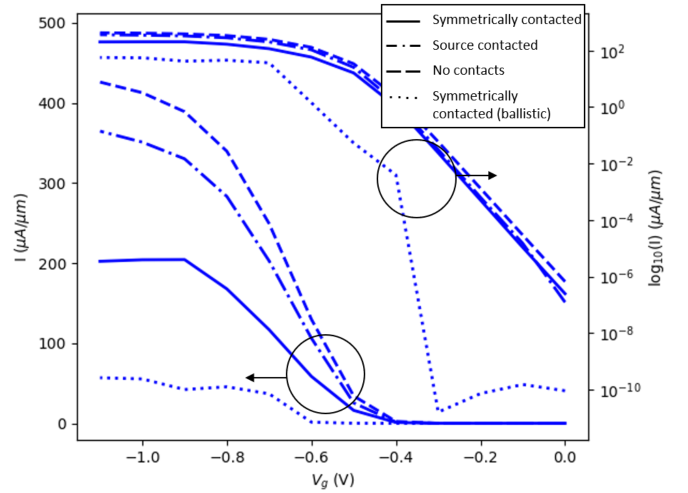

Fig. 2. IV curves of a $14\,\mathrm{nm}$ channel NbS_2 top contacted WS_2 transistor as a function of the gate bias for $V_{dd} = 0.15\,\mathrm{V}$. Three contact configurations are considered: explicit metal contact simulation at both source and drain as denoted in 1 (b) (symmetrically contacted), explicit metal contact simulation at the source and ohmic contact at the drain (source contacted) and ohmic contacts at both source and drain without any explicit metal parts (no contacts). For the first case, both a dissipative simulation and a ballistic simulation with scattering mechanisms disabled were performed.

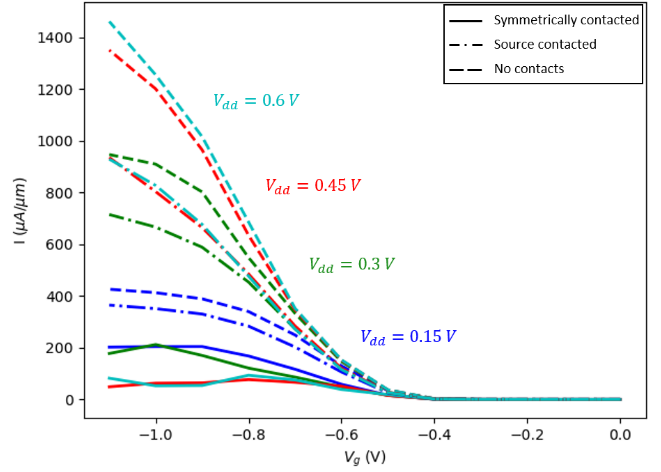

Fig. 3. IV curves for the same devices as in Fig. 2 for several source-drain biases.

carriers the required energy to cross the channel barrier, as demonstrated by the current spectra in Fig. 4 (a) and 4 (b). Hence, the symmetrically contacted device is constrained by the same thermionic limit as the reference without cold metal contacts. The source contacted reference achieves a marginally better S_{th} of $55.5\,\mathrm{mV/dec}$, but as this is mostly due to the lower current of one single bias point, this could be attributed to numerical convergence issues as well.

Additionally, Fig. 2 shows that the metal contacts introduce a contact resistance and hence, a drop in the ON current, I_{ON}. As the Schottky barrier height is found to be very low, this is attributed to the tunneling barrier of the van der

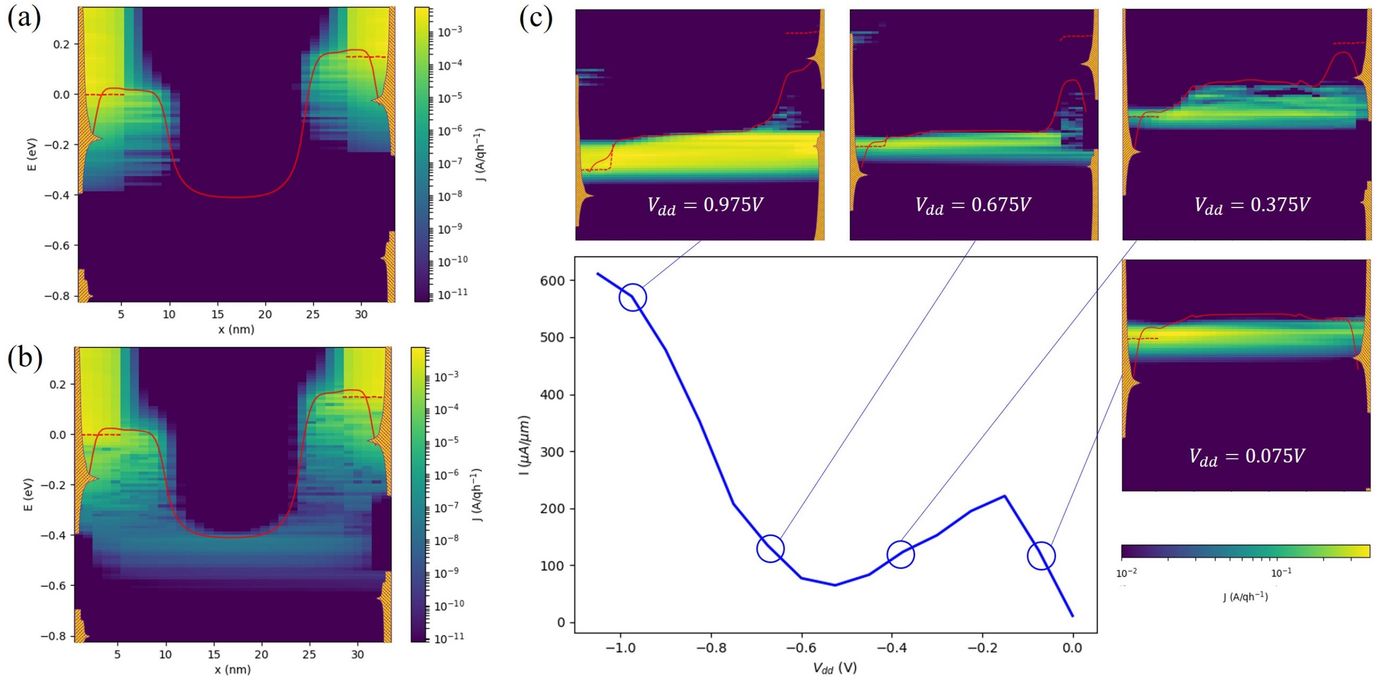

Fig. 4. (a) en (b) current spectra as a function of the position along the transport direction for the symmetrically contacted transistor in Fig. 1 (a) for $V_{dd} = 0.15\,\mathrm{V}$, obtained with, respectively, a ballistic and dissipative simulation. The hatched orange regions at the the edges of the spectra denote the density of states of the bulk-like NbS_2 contacts. The red dashed and full line are respectively the Fermi level in NbS_2 and the top of the valence band in WS_2. (c) ON current of a symmetrically contacted NbS_2-WS_2 transistor as a function of source-drain bias. The current has a local minimum at $V_{dd} = 0.5\,\mathrm{V}$. Current spectra, similar to the ones in (a) en (b), are shown for several values of V_{dd}, demonstrating the overlap of the injection window at the source with the band gap at the drain.

Waals gap. It is apparent that the degradation of I_{ON} is much more severe in the ballistic limit. Thus, even though scattering negates the benefits of using cold metals, it also helps in preserving sufficient ON current. The source contacted device shows only a limited decrease of I_{ON}. However, for the symmetrically contacted transistor, I_{ON} decreases much more drastically, even with scattering incorporated. Additionally, Fig. 3 shows that I_{ON} decreases when V_{dd} is increased for the symmetrically contacted device. This is attributed to the fact that the energy at which carriers are injected at the source comes to lie in the small band gap of the NbS_2 at the drain, when the source-drain bias is increased. Hence, there are no available states at the drain for the carriers to travel to and the carriers are required to scatter before being extracted by the drain. However, as this scattering process is slow, the ON current is degraded for source-drain biases for which scattering is a requirement.

The phenomenon of decreased injection window and extraction window overlap is denoted in Fig 4 (c). One can clearly see a linear increase of I_{ON} with increasing source-drain bias for low source-drain biases. The current then starts to decrease as the injection window moves in the small band gap at around $V_{dd} = 0.3\,\mathrm{V}$. Due to the band gap of interest being small, a further increase of V_{dd} causes I_{ON} to increase again at around $V_{dd} = 0.675\,\mathrm{V}$. For these stronger source-drain biases there is overlap of the injection window with lower lying states below the band gap. This is, however, unique to NbS_2 and does not necessarily hold for other cold metals which can have larger band gaps. It should be noted that for low source-drain biases, there are states available at the drain for extraction of carriers. Therefore, there is no evident reason why scattering should be required to preserve ON current for these low values of V_{dd}. Hence, we do not exclude the possibility that the degradation of ON current in the ballistic limit is not due the cold metal characteristic of the metal, but a result of a metal top contact in general. Further discussion of this point is however beyond the scope of this paper.

Finally, 2D materials and cold metals are candidates for ultra-scaled devices due to, respectively, their predicted excellent electrostatic control and low subthreshold swings. Especially the influence of cold metals on the scaling of devices is of utmost importance, as shorter devices generally behave more ballistically. However, the discussion above showed that NbS_2-WS_2 devices in the ballistic limit show a severe degradation of the ON current. Therefore, we performed a simulation of a shortened symmetrically contacted device, with a channel length of only $5\,\mathrm{nm}$ and source-drain extensions with reduced lengths of $2.3\,\mathrm{nm}$ for the part not underneath the NbS_2 contact. For the source-drain bias, $V_{dd} = 0.15\,\mathrm{V}$ was chosen to prevent issues concerning the non-overlap of injection and extraction window. The resulting IV curves are shown in Fig. 5. It is clear that the ON current is not degraded significantly more than the $14\,\mathrm{nm}$ device. Hence, the benefits of electron-phonon scattering are preserved for short devices.

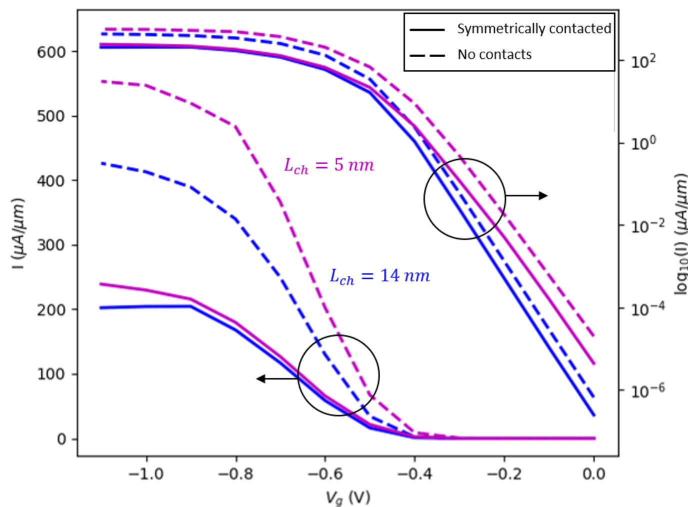

Fig. 5. IV curves of the transistor shown in Fig. 1 and a shorter device with a channel length of $5\,\mathrm{nm}$ and half length source-drain extensions.

Additionally, it can be seen that the symmetrically contacted device preserves a marginally better S_{th} of $65.5\,\mathrm{mV/dec}$ compared to $68\,\mathrm{mV/dec}$ for the pure WS_2 reference. Hence, the subthreshold swing degradation for short devices due to reduced electrostatic control can be partially countered by the use of cold metals.

IV. Conclusion

We showed that the benefits of cold metals, observed in the ballistic limit, are negated by electron-phonon interactions. Scattering processes allow injected carriers to obtain enough energy to cross the channel barrier. Symmetrically contacted devices are therefore also constrained by the thermionic limit of $S_{th} = 60\,\mathrm{mV/dec}$. Asymmetric devices with a cold metal contact at the source only can achieve a lower value for S_{th} but only marginally so and this lower value could be the result of numerical convergence issues. Additionally, the use of cold metals can give rise to a significant ON current degradation. Scattering can partially, but not fully, restore this ON current. Scattering thus negates the benefits of cold metal contacts but is nevertheless required for adequate device performance. Even with scattering processes, the ON current degradation increases with increased source-drain bias due to limited overlap of the energies at which carriers are injected and the energies at which states are available for extraction at the drain. For the case of NbS_2 specifically, this process halts and the ON current starts to increase again beyond a certain threshold for V_{dd} due to the availability of states below the band gap. For shorter devices, expected to behave closer to the ballistic limit, cold metals can partially offset the subthreshold swing degradation due to reduced electrostatic control, although only marginally so. However, they do not suffer from the ON current degradation found for fully ballistic simulations.

References

[1] F. Schwierz, J. Pezoldt, and R. Granzner, "Two-dimensional materials and their prospects in transistor electronics," *Nanoscale*, vol. 7, no. 18, pp. 8261–8283, 2015.

[2] D. Logoteta, Q. Zhang, and G. Fiori, "What can we really expect from 2d materials for electronic applications?," in *72nd Device Research Conference*, IEEE, 2014.

[3] M. Chhowalla, D. Jena, and H. Zhang, "Two-dimensional semiconductors for transistors," *Nature Reviews Materials*, vol. 1, no. 11, p. 16052, 2016.

[4] J. Kang, W. Cao, X. Xie, D. Sarkar, W. Liu, and K. Banerjee, "Graphene and beyond-graphene 2d crystals for next-generation green electronics," in *Micro-and Nanotechnology Sensors, Systems, and Applications VI*, vol. 9083, p. 908305, International Society for Optics and Photonics, 2014.

[5] A. Afzalian, J.-P. Colinge, and D. Flandre, "Physics of gate modulated resonant tunneling (RT)-FETs: Multi-barrier MOSFET for steep slope and high on-current," *Solid-State Electronics*, vol. 59, pp. 50–61, May 2011.

[6] F. Liu, "Switching at less than 60 mv/decade with a "cold" metal as the injection source," *Phys. Rev. Applied*, vol. 13, p. 064037, 2020.

[7] A. Afzalian and G. Pourtois, "Atomos: An atomistic modelling solver for dissipative dft transport in ultra-scaled hfs2 and black phosphorus mosfets," in *2019 International Conference on Simulation of Semiconductor Processes and Devices (SISPAD)*, pp. 1–4, 2019.

[8] M. Paulsson, "Non equilibrium green's functions for dummies: Introduction to the one particle negf equations," *arXiv preprint cond-mat/0210519*, 2002.

[9] N. Marzari, A. A. Mostofi, J. R. Yates, I. Souza, and D. Vanderbilt, "Maximally localized wannier functions: Theory and applications," *Reviews of Modern Physics*, vol. 84, no. 4, pp. 1419–1475, 2012.

[10] A. Afzalian, "Ab initio perspective of ultra-scaled CMOS from 2d-material fundamentals to dynamically doped transistors," *npj 2D Materials and Applications*, vol. 5, no. 1, 2021.

[11] P. Giannozzi, S. Baroni, N. Bonini, M. Calandra, R. Car, C. Cavazzoni, D. Ceresoli, G. L. Chiarotti, M. Cococcioni, I. Dabo, A. D. Corso, S. de Gironcoli, S. Fabris, G. Fratesi, R. Gebauer, U. Gerstmann, C. Gougoussis, A. Kokalj, M. Lazzeri, L. Martin-Samos, N. Marzari, F. Mauri, R. Mazzarello, S. Paolini, A. Pasquarello, L. Paulatto, C. Sbraccia, S. Scandolo, G. Sclauzero, A. P. Seitsonen, A. Smogunov, P. Umari, and R. M. Wentzcovitch, "QUANTUM ESPRESSO: a modular and open-source software project for quantum simulations of materials," *Journal of Physics: Condensed Matter*, vol. 21, no. 39, p. 395502, 2009.

[12] A. Afzalian, E. Akhoundi, G. Gaddemane, R. Duflou, and M. Houssa, "Advanced DFT-NEGF transport techniques for novel 2-d material and device exploration including hfs_2/wse_2 van der waals heterojunction TFET and wte_2/ws_2 metal/semiconductor contact," *IEEE Transactions on Electron Devices*, pp. 1–8, 2021. doi:10.1109/TED.2021.3078412.